

Experimental evidence of Er^{3+} ions reduction in the radiation-induced degradation of erbium-doped silica fibers

Yasmine Mebrouk,^{1,*} Franck Mady,¹ Mourad Benabdesselam,¹ Jean-Bernard Duchez,¹ and Wilfried Blanc¹

¹Université Nice Sophia Antipolis, CNRS, Laboratoire de Physique de la Matière Condensée, UMR 7336, 06100 Nice, France.

The gain of erbium doped fiber amplifiers is damaged by irradiation partly because of creation of color centers responsible of excess absorption at pump and signal wavelengths. Based on the combination of thermally stimulated luminescence and spectrophotometry, this letter demonstrates that a part of the gain loss should be associated with the reduction of the density of Er^{3+} ions by irradiation.

OCIS codes: (0.60.2410) Fibers, erbium; (350.5610) Radiations; (060.2320) Fiber optics amplifiers and oscillators.

Erbium-doped fibers (EDF) have proved to be very attractive for a large domain of applications such as super-luminescent sources, lasers, or optical signals amplifiers emitting around $1.55 \mu\text{m}$. In recent years, EDF have been thought to be employed in harsh environments (nuclear reactor, space communications,...) [1]. However, ionizing radiations damage EDF and lead to the degradation of gain and signal transmission [1, 2]. It is admitted that the gain degradation is due to the creation of color centers (CC) that are responsible for a so-called radiation-induced attenuation (RIA), that is excess loss at signal and pump wavelength notably [3–5]. If the absorption and emission cross sections of Er^{3+} ions are not modified by irradiation [4], these degradations can be attributed to the combination of two effects: (i) pump absorption by CC [3] reduces the pump power available for population inversion therefore the gain is damaged. (ii) Signal absorption by CC. For instance, phosphorus doping introduces absorbing defects near 0.8 eV (1550 nm) that leads to a decrease of the transmitted signal power during irradiation. Aside from the role of CC, the direct involvement of Er^{3+} ions in the gain degradation has not been investigated so far, probably because it has been ruled out based on hasty conclusions [4–6]. However, a recent work by Likhachev *et al.* [7] concluded indirectly that Er^{3+} ions may contribute to the gain degradation by comparing two germanosilicates (irradiated in identical conditions) with the same amount of GeO_2 but two different concentrations of Er_2O_3 . These authors found a higher RIA level in the fiber containing more erbium. Based on the coupling between thermally stimulated luminescence (TSL) and spectrophotometry measurements, we demonstrate in a much more straightforward way that the gain degradation is partly due to the reduction of the density of Er^{3+} ions.

Samples consisted of preform discs with 0.5 mm core radius and 1 mm thickness and also of corresponding fibers. Preforms were fabricated by the conventional modified chemical vapour deposition (MCVD) process and solution doping technique and drawn in our laboratory. Measurements in the UV-visible were carried

out on preform samples to avoid multimodal propagation artifacts in fibers. Near infra-red (NIR) measurements were made on fibers with an Anritsu optical spectrum analyzer. We investigated three silica-based preform compositions: one with erbium only (pEr), two with different concentrations of aluminum and the same amount of erbium (pAl1:Er, pAl2:Er), and one with germanium and erbium (pGe:Er). Density of Er^{3+} ions is about $1.5 \times 10^{25} \text{m}^{-3}$ for all samples. pAl1:Er and pAl2:Er contain 0.25 and 1.37 at.% of Al, respectively. pGe:Er contains 0.15 at.% of Ge. Irradiations were carried out with 45 kV x-rays from a copper-anode tube at $1.2 \text{ krad min}^{-1}(\text{SiO}_2)$. Absorption measurements were performed by a PerkinElmer Lambda 1050 spectrophotometer. Both irradiations and absorption measurements were conducted at room temperature (RT). TSL of irradiated samples was measured by a Harshaw TLD 3500 reader. TSL reveals all the optically active centers and defects whose valence state has been modified by irradiation. It consists of photons emitted upon radiative recombination of "detrapped" carriers with carriers of opposite polarity on reduced/oxidized centers (recombination centers). This standard interpretation framework of TSL, based on trapping and recombination mechanisms, has been shown to be a proper basis to explain the RIA build-up and bleaching [8, 9]. After radiation exposure, samples are heated up linearly ($2 \text{ }^\circ\text{C s}^{-1}$) from RT up to $600 \text{ }^\circ\text{C}$ and carriers are thermally released from traps of increasing depths. The TSL is plotted as a function of temperature to give "glow curves" that reflect the energy distribution of trapped states generated by irradiation. Glow curves exhibit "peaks". Each trapping level gives rise to a single peak (the deeper the trap, the higher the peak temperature). TSL spectra acquired at each temperature with an optical multi-channel analyzer allow the identification of photoionized luminescent centers.

Normalized TSL glow curves obtained after x-ray irradiation ($300 \text{ krad}(\text{SiO}_2)$) of our samples are shown in Fig. 1. They all present three main broad peaks indicating that three groups of traps are populated by irradiation. Peak 1 lays between 50 and $150 \text{ }^\circ\text{C}$, peak 2 and 3 are in the $200\text{-}300 \text{ }^\circ\text{C}$ and $350\text{-}450 \text{ }^\circ\text{C}$ range respectively. For the pEr and pAl1:Er samples, peak 2 is not intense enough to be separated clearly from the broad first peak.

* Corresponding author: mebrouk@unice.fr

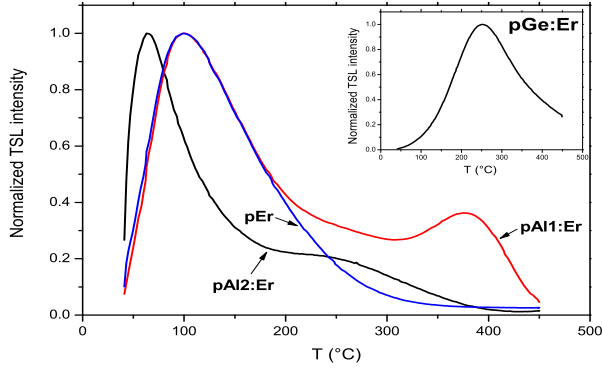


FIG. 1. Normalized TSL intensity as function of temperature for pAl1:Er, pAl2:Er, pEr preform samples. Inset: pGe:Er sample.

A similar peak at 250 ° is found in pGe:Er but in this case it is attributed to the recombination of released electrons on ionized germanium lone pair center (GLPC) [10–12].

Fig. 2 represents the spectral analysis of the TSL emissions. Spectra were measured at 100 ° C but the same luminescence features are observed throughout the temperature range. All samples show green emission bands at 525 and 547 nm corresponding respectively to transitions from ${}^2\text{H}_{11/2}$ and ${}^4\text{S}_{3/2}$ to the ground state level ${}^4\text{I}_{15/2}$ of Er^{3+} ions. In the case of the Ge-doped sample (pGe:Er, inset), one can see the well-known intense blue-violet emission of GLPC recombination [10, 13]. In addition, one can distinguish a weak Er^{3+} emission at 404 and 474 nm in the case of pAl:Er and pEr samples. These features probably exist in the spectrum of pGe:Er but might be hidden by the very intense emission of GLPC. Trap emptying during the TSL readout is followed by recombination of released carriers, which is accompanied by emissions of Fig. 2. Since this TSL mechanism leads to the thermal bleaching of the samples (see below), it must consist of the reverse processes to those operating during irradiation, i.e. ionization leading to generation of free carriers and traps filling responsible for darkening and RIA. The presence of the emission of Er^{3+} ions indicates that carriers released from TSL trap recombine with previously ionized centers to form an excited Er^{3+} ions that subsequently de-excites. Somehow, this means that erbium ions have been ionized by irradiation and thus that Er^{3+} ions have been lost. To correlate the TSL glow curves with absorption measurements, thermal bleaching of RIA was examined according to the following procedure: after the optical absorption of the pristine preforms core was measured, samples were irradiated with x-rays (300 krad (SiO_2)). The absorption of the irradiated core was measured and then the sample was heated up to $T_{\text{stop}} = 50$ ° C at 2 ° C s^{-1} (the same heating rate as in TSL readouts to allow comparison). The new core absorption was measured after cooling down at room temperature. Then, the sample was heated up to $T_{\text{stop}} = 100$ ° C and the new core absorption was measured, etc ... The partial core bleaching within 50 ° C slots was monitored by considering T_{stop}

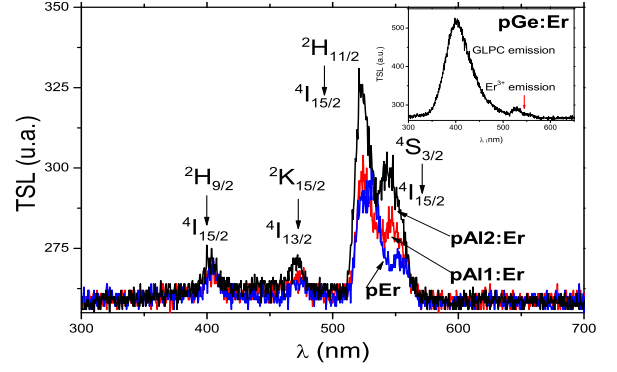


FIG. 2. Normalized TSL spectra after x-rays irradiation (300 krad) at 100 ° C for Al:Er-, Er- and Ge:Er- (inset) doped core preforms.

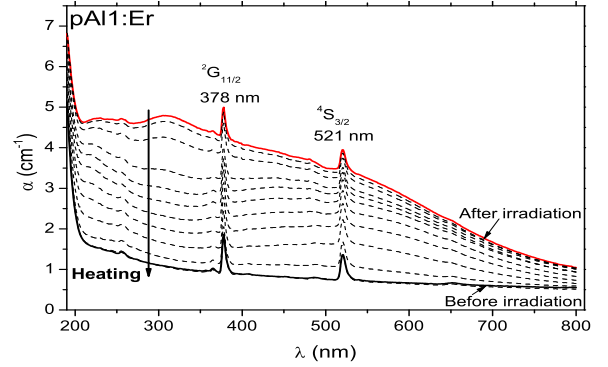


FIG. 3. Absorption spectra before and after x-rays irradiation (300 krad) for Al:Er-doped core preforms. Dashed curves : absorption after heating up from RT up to 600 ° C by steps of 50 ° C.

= 150, 200, ... up to 600 ° C. Absorption coefficients α before and after x-ray irradiation of pAl1:Er core sample are plotted in Fig. 3. Dashed curves correspond to absorption spectra. Er^{3+} ground state absorption transitions to ${}^2\text{G}_{11/2}$ and ${}^4\text{S}_{3/2}$ levels are located at 378 and 521 nm, respectively. Core absorption increases in the UV-visible range after irradiation. After heating up to 600 ° C we observe the total recovery of RIA and TSL readouts do not provide any signal. Therefore the total emptying of TSL traps well corresponds to the complete RIA bleaching. Absorption by other samples (not shown here) exhibits the same darkening/bleaching behavior. The difference between the post- and pre-irradiation absorption spectra (*i.e.* RIA) is plotted in Fig 4. RIA plots reveal the formation of absorbing centers characterized by overlapping absorption bands lying from UV to visible (for instance, AlE' absorption band at 300 nm [14], Al-OHC at 540 nm and NBOHC at 620 nm [15]). At the 378 and 521 nm Er^{3+} absorption wavelengths we notice two "holes" corresponding to a decrease of Er^{3+} ions absorption by irradiation. The depth of these two "holes" depends on the codoping element. It was found to increase with the Al concentration but is less pronounced in the Ge-doped sample. Since thermal bleaching experiments are done at the same heating rate as TSL readouts,

the Gaussian deconvolution of absorption spectra at each T_{stop} (Fig. 3) may allow us to compare the temperature-resolved bleaching of each gaussian component with TSL glow curves and thus to assign related defects to TSL peaks and traps. This task is actually very hard, due to the multiplicity of the deconvolution solutions notably. We analyzed the variation of Er^{3+} absorption ($\alpha(\text{Er}^{3+})$)

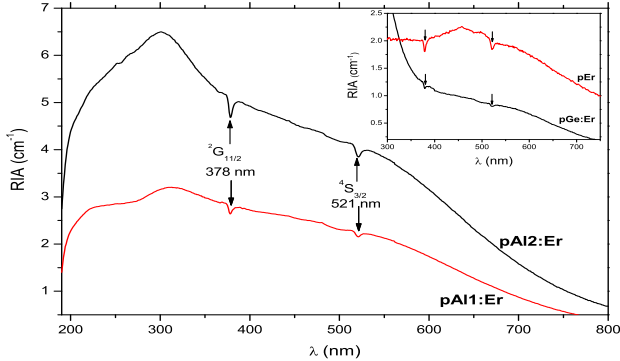


FIG. 4. Radiation induced absorption (difference between post- and pre- radiation absorption data) for pAl1:Er and pAl2:Er sample and for pEr and pGe:Er in the inset.

at 378 and 521 nm by extracting the corresponding bands from spectra of Fig. 3 using the best-suited interpolation of each data spectrum; the obtained result is shown in Fig 5-a. Clearly, the 378 and 521 nm bands areas are decreased by irradiation. Then, absorption recovers gradually with increasing T_{stop} . The change of α can be due to a variation either in the absorption cross-section σ_{abs} or in the density of erbium ions N . It has been argued that Er^{3+} ions absorption and emission cross-sections are not affected by γ -radiations [4]. Our results also support this finding in case of x-ray irradiation. Indeed, normalized curves of Fig 5-b show that all spectra exhibit the same shape with identical FWHM (0.03 eV at 521 nm and 0.04 eV at 378 nm) before and after irradiation and throughout the thermal recovery protocol. Measurements between 1400 and 1600 nm on Al:Er-doped preforms and fibers (made in our laboratory or commercial), reported in Fig. 6, confirm the decrease of $\alpha(\text{Er}^{3+})$ observed in UV-visible range. The absorption level is reduced after irradiation and normalization of spectra in insets again shows that the band shape does not change after irradiation. Therefore, we conclude that the absorption cross section σ_{abs} does not change and the decrease in $\alpha(\text{Er}^{3+})$ after x-ray irradiation is due to the decrease of the density N of Er^{3+} ions. One can underline that the drawing process has no impact on this result. The direct contribution of Er^{3+} ions in the gain degradation has been dismissed to date [4, 6]. Obviously a significant amount of Er^{3+} ions is lost by irradiation.

Fig. 7 illustrates the correlation between the TSL curves and the recovery curves of Er^{3+} absorption lines for pAl1 (and 2):Er samples. Although not reported here, similar behaviors have been observed for other samples. The ordinate of each point corresponds to the percentage recovery in the 50 °C interval. For example: the point at

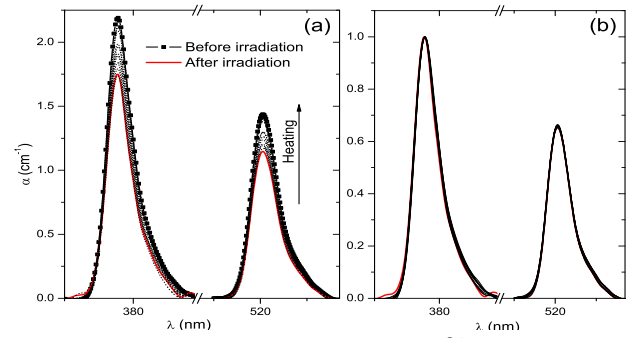


FIG. 5. Extracted 521 and 378 nm Er^{3+} absorption band : (a) before and after irradiation and for all T_{stop} of thermal recovery. (b): The same normalized with respect to the maximum.

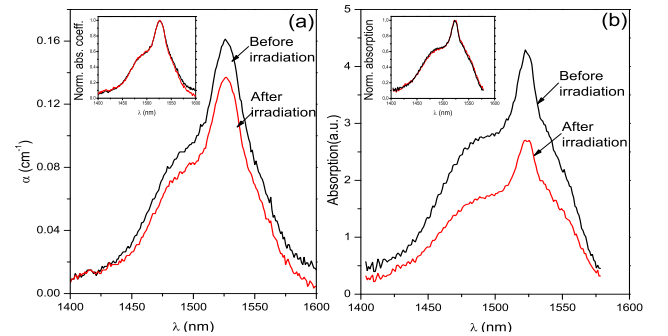


FIG. 6. Near infrared absorption of pre- and post-irradiated Al:Er doped preform (a) and for Liekki Er-80 fibre (b). Insets show the normalized data.

325 °C corresponds to the difference between area under curves at 350 °C and 300 °C normalized by the RIA at the given wavelength. Recovery plots at 378 and 521 nm have been deduced from Fig. 5. They should be identical. In practice, they roughly show similar trends. Discrepancies are mainly due to the weak recovery within each 50 °C slot, so differences between spectra at two successive T_{stop} are highly inaccurate. The recovery of Er^{3+} ions follows the trap emptying depicted by the TSL curve, except for the first peak component below 100 °C which is apparently poorly involved in the process (carriers released from the corresponding traps do not strongly take part in the re-formation of Er^{3+} ions so additional TSL emissions probably exist out of the wavelength window of our spectral measurements (Fig. 2).

A possible explanation of the reduction of Er^{3+} density after irradiation is a valence change to divalent ions. The change in erbium ionization state is as likely as in the case of other rare earth ions. Europium and ytterbium are known to exist in divalent state in oxide glasses; reduction of these rare earth ions by irradiation is possible [8, 16]. Divalent erbium Er^{2+} was observed in CaF_2 [17] and has been obtained by synthetic methods [18] but it has never been reported in an oxide glass. The radiation induced attenuation mechanism in Er-doped silica could be the same as in Yb-doped [8]. According to TSL and absorption measurements, we can propose the following mechanism: under irradiation Er^{3+} ions are reduced to

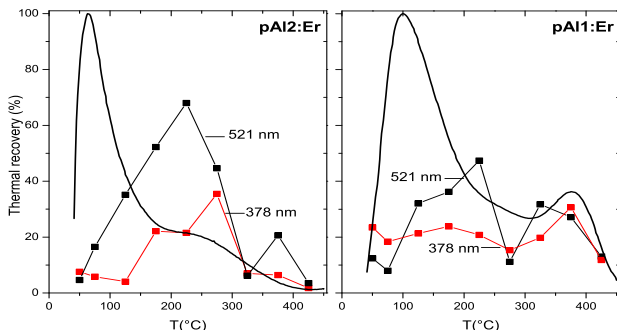


FIG. 7. Thermal recovery of the absorption for pAl1:Er and pAl2:Er preforms at 378 and 521 nm. Normalized TSL curves are also shown for comparison.

the form Er^{2+} by trapping an electron, a hole is consequently captured to form trapped hole centers (AlE', Al-OHC, NBOHC [13, 14]) that obviously contribute to RIA (Fig 4). Upon thermal or optical excitation, radiation induced trapped holes are released and recombine to reform Er^{3+} ions. Based on the variation in Er^{3+} ions absorption bands, the density of ions reduced after irradiation (300 krad) is about 20% for pAl1:Er, 32% for pAl2:Er (with more Al) and 12% for pGe:Er sample. In the case of Ge-codoping, the reduction is smaller for the same density of Er^{3+} ions. It could be explained as follows: Ge introduces a huge amount of electron traps (Ge (1) and Ge(2)) [13] that are in competition with Er^{3+} for

trapping electrons and could trap more electrons than Er^{3+} . By contrast, Al-doping introduces hole traps and favors electrons trapping on Er^{3+} ions. Moreover, Al and Er ions are well-known to be closely located which may favor the recombination process [19]. In small signal conditions, the gain loss resulting from the conversion of erbium ions should be proportional to the conversion rate, say in the 10-35 % range (at 300 Gy) according to our data. For 30 dB amplifier, e.g., the gain should be decreased by 3-10 dB due to the radiation effect on erbium ions (out of RIA). This should be compared to typical RIA levels reported in literature, i.e. about 20 dB for a 2m-long conventional aluminosilicate amplifier at 1550 nm and about 0.4 dB for radiation-hardened fibers, in same conditions [7, 20]. Therefore the loss in Er^{3+} ions can have a non-negligible impact on the gain degradation, in addition to RIA. This contribution will be more critical in fibers exhibiting low RIA levels due to optimization of the core compositions [7, 20]. It could even determine the gain degradation in highly RIA-resistant fibers. Complementary characterizations are of course needed to estimate the consequences of the basic result demonstrated in this letter.

This work, including the PhD thesis of Yasmine ME-BROUK, has been funded by the AirbusGroup foundation under grant # 098-AO11-1108. The authors gratefully acknowledge this support.

-
- [1] S. Girard, J. Kuhnenn, A. Gusarov, B. Brichard, M. Van Uffelen, Y. Ouerdane, A. Boukenter, C. Marcandella, *IEEE Trans. Nucl. Sci.*, **60**, 2015 (2013)
- [2] M. Hill, R. Gray, J. Hankey, A. Gillooly, In *OFC Technical Digest March 14-16, 2014*
- [3] T.S. Rose, D. Gunn, G. C. Valley, *J. Light. Technol.*, **19**, 1918 (2001)
- [4] B. Tortech, M. Van Uffelen, A. Gusarov, Y. Ouerdane, A. Boukenter, J. P. Meunier, F. Berghmans, H. Thienpont, *J. Non Cryst. Solids*, **353**, 477 (2007)
- [5] B.P. Fox, K. Simmons-Potter, D. A.V. Kliner, S. W. Moore, *J. Non Cryst. Solids*, **378**, 79 (2013)
- [6] S. Girard, A. Laurent, E. Pinsard, T. Robin, B. Cadier, M. Boutillier, C. Marcandella, A. Boukenter, Y. Ouerdane, *Opt. Lett.*, **39**, 2541 (2014)
- [7] M. E. Likhachev, M. M. Bubnov, K. V. Zotov, A. L. Tomashuk, D. S. Lipatov, M. V. Yashkov, A. N. Guryanov, *J. Light. Technol.*, **31**, 749 (2013)
- [8] F. Mady, M. Benabdesselam, W. Blanc, *Opt. Lett.*, **35**, 3541 (2010)
- [9] F. Mady, M. Benabdesselam, J. B. Duchez, Y. Mebrouk, S. Girard, *IEEE Trans. Nucl.Sci.*, **60**, 4341 (2013)
- [10] M. Fujimaki, T. Watanabe, T. Katoh, T. Kasahara, N. Miyazaki, Y. Ohki, H. Nishikawa, *Phys. Rev. B*, **57**, 3920 (1998)
- [11] M. Benabdesselam, F. Mady, S. Girard, Y. Mebrouk, J. B. Duchez, M. Gaillardin, P. Paillet, *IEEE Trans. Nucl.Sci.*, **60**, 4251 (2013)
- [12] M. Benabdesselam, F. Mady, S. Girard, *J. Non Cryst. Solids*, **360**, 9 (2013)
- [13] D.L. Griscom, *Opt. Mater. Express*, **1**, 400 (2011)
- [14] H. Hosono, H. Kawazoe, *Nucl. Instrum. Methods B*, **91**, 395 (1994)
- [15] L. Skuja, *J. Non Cryst. Solids*, **239**, 16 (1998)
- [16] S. Rydberg, M. Engholm, *Optics Express*, **21**, 6681 (2013)
- [17] J.L. Merz and P.S. Pershan, *Phys. Rev.*, **162**, 217 (1967)
- [18] M.R. MacDonald, J. E. Bates, M. E. Fieser, J. W. Ziller, F. Furche, W. J. Evans, *J. Am. Chem. soc.*, **134**, 8420 (2012)
- [19] A. Monteil, S. Chaussedent, G. Alombert-Goget, N. Gaumer, J. Obriot, S.J.L. Ribeiro, Y. Messaddeq, A. Chiasera, M. Ferrari, *J. Non-Cryst. Solids*, **348**, 44 (2004)
- [20] K. V. Zotov, M. E. Likhachev, A. L. Tomashuk, A. F. Kosolapov, M. M. Bubnov, M. V. Yashkov, A. N. Guryanov, and E. M. Dianov, *IEEE Photon. Technol. Lett.* 20(17), 14761478 (2008).

-
- [1] S. Girard, J. Kuhnenn, A. Gusarov, B. Brichard, M. Van Uffelen, Y. Ouerdane, A. Boukenter, C. Marcandella, "Radiation effects on silica-based optical fibers: recent advances and future challenges", *IEEE Trans. Nucl. Sci.*, **60**, 2015 (2013)
- [2] M. Hill, R. Gray, J. Hankey, A. Gillooly, "Fibers for multi-channel erbium doped amplifiers in optical space communications", In *OFC Technical Digest* March 14-16, 2014
- [3] T.S. Rose, D. Gunn, G. C. Valley, "Gamma and proton radiation effects in erbium-doped fiber amplifiers: active and passive measurements", *J. Light. Technol.*, **19**, 1918 (2001)
- [4] B. Tortech, M. Van Uffelen, A. Gusarov, Y. Ouerdane, A. Boukenter, J. P. Meunier, F. Berghmans, H. Thienpont, "Gamma radiation induced loss in erbium doped optical fibers", *J. Non Cryst. Solids*, **353**, 477 (2007)
- [5] B.P. Fox, K. Simmons-Potter, D. A.V. Kliner, S. W. Moore, "Effect of low-earth orbit space on radiation-induced absorption in rare-earth-doped optical fibers", *J. Non Cryst. Solids*, **378**, 79 (2013)
- [6] S. Girard, A. Laurent, E. Pinsard, T. Robin, B. Cadier, M. Boutillier, C. Marcandella, A. Boukenter, Y. Ouerdane, "Radiation-hard erbium optical fiber and fiber amplifier for both low- and high-dose space missions", *Opt. Lett.*, **39**, 2541 (2014)
- [7] M. E. Likhachev, M. M. Bubnov, K. V. Zotov, A. L. Tomashuk, D. S. Lipatov, M. V. Yashkov, A. N. Guryanov, "Radiation resistance of Er-doped silica fibers: effect of host glass composition", *J. Light. Technol.*, **31**, 749 (2013)
- [8] F. Mady, M. Benabdesselam, W. Blanc, "Thermoluminescence characterization of traps involved in the photodarkening of ytterbium-doped silica fibers", *Opt. Lett.*, **35**, 3541 (2010)
- [9] F. Mady, M. Benabdesselam, J. B. Duchez, Y. Mebrouk, S. Girard, "Global view on dose rate effects in silica-based fibers and devices damaged by radiation-induced carrier trapping", *IEEE Trans. Nucl.Sci.*, **60**, 4341 (2013)
- [10] M. Fujimaki, T. Watanabe, T. Katoh, T. Kasahara, N. Miyazaki, Y. Ohki, H. Nishikawa, "Structures and generation mechanisms of paramagnetic centers and absorption bands responsible for Ge-doped SiO₂ optical-fiber gratings", *Phys. Rev. B*, **57**, 3920 (1998)
- [11] M. Benabdesselam, F. Mady, S. Girard, Y. Mebrouk, J. B. Duchez, M. Gaillardin, P. Paillet, "Performance of Ge-doped optical fiber as a thermoluminescent dosimeter", *IEEE Trans. Nucl.Sci.*, **60**, 4251 (2013)
- [12] M. Benabdesselam, F. Mady, S. Girard, "Assessment of Ge-doped optical fibre as a TL-mode detector", *J. Non Cryst. Solids*, **360**, 9 (2013)
- [13] D.L. Griscom, "On the natures of radiation-induced point defects in GeO₂-SiO₂ glasses: reevaluation of a 26-year-old ESR and optical data set", *Opt. Mater. Express*, **1**, 400 (2011)
- [14] H. Hosono, H. Kawazoe, *Nucl. Instrum. Methods B*, "Radiation-induced coloring and paramagnetic centers in synthetic SiO₂:Al glasses", **91**, 395 (1994)
- [15] L. Skuja, *J. Non Cryst. Solids*, "Optically active oxygen-deficiency-related centers in amorphous silicon dioxide", **239**, 16 (1998)
- [16] S. Rydberg, M. Engholm, "Experimental evidence for the formation of divalent ytterbium in the photodarkening process of Yb-doped fiber lasers", *Optics Express*, **21**, 6681 (2013)
- [17] J.L. Merz and P.S. Pershan, "Charge Conversion of Irradiated rare-earth ions in calcium fluoride", *Phys. Rev.*, **162**, 217 (1967)
- [18] M.R. MacDonald, J. E. Bates, M. E. Fieser, J. W. Ziller, F. Furche, W. J. Evans, "Expanding Rare-Earth Oxidation State Chemistry to Molecular Complexes of Holmium(II) and Erbium(II)", *J. Am. Chem. soc.*, **134**, 8420 (2012)
- [19] A. Monteil, S. Chaussedent, G. Alombert-Goget, N. Gaumer, J. Obriot, S.J.L. Ribeiro, Y. Messaddeq, A. Chiasera, M. Ferrari, "Clustering of rare earth in glasses, aluminum effect: experiments and modeling", *J. Non-Cryst. Solids*, **348**, 44 (2004)
- [20] K. V. Zotov, M. E. Likhachev, A. L. Tomashuk, A. F. Kosolapov, M. M. Bubnov, M. V. Yashkov, A. N. Guryanov, and E. M. Dianov, "Radiation resistant Er-doped fibers: optimization of pump wavelength", *IEEE Photon. Technol. Lett.* 20(17), 14761478 (2008).